ISSN 1674-1056
http://cpb.iphy.ac.cn
http://iopscience.iop.org/cpb
中国物理 B
Chinese Physics
中国物理
Chinese Physics B

Confinement-induced modulation of elastic properties of nano-confined fluids in slit pore

Zong-Li Sun(孙宗利), Yan-Shuang Kang(康艳霜), Yan-Mei Kang(康艳梅)

Citation: Chin. Phys. B . 2019, 28(3): 036102. **doi:** 10.1088/1674-1056/28/3/036102
Journal homepage: http://cpb.iphy.ac.cn; http://iopscience.iop.org/cpb

What follows is a list of articles you may be interested in

Effects of temperature and point defects on the stability of C15 Laves phase in iron: A molecular dynamics investigation

Hao Wang(王昊), Ning Gao(高宁), Guang-Hong Lü(吕广宏), Zhong-Wen Yao(姚仲文)
Chin. Phys. B . 2018, 27(6): 066104. **doi:** 10.1088/1674-1056/27/6/066104

Bandgap engineering to tune the optical properties of $Be_xMg_{1-x}X$ (X=S, Se, Te) alloys

B Sabir, N A Noor, M Rashid, Fasih Ud Din, Shahid M Ramay, Asif Mahmood
Chin. Phys. B . 2018, 27(1): 016101. **doi:** 10.1088/1674-1056/27/1/016101

Density functional study on the pressure profile of the inhomogeneous fluid mixture

Yanshuang Kang(康艳霜), Yanmei Kang(康艳梅), Zongli Sun(孙宗利), Yushan Li(李玉山), Shanshan Tan(檀姗姗)
Chin. Phys. B . 2017, 26(8): 086101. **doi:** 10.1088/1674-1056/26/8/086101

High-pressure structure and elastic properties of tantalum single crystal: First principles investigation

Jian-Bing Gu(顾建兵), Chen-Ju Wang(王臣菊), Wang-Xi Zhang(张旺玺), Bin Sun(孙斌), Guo-Qun Liu(刘国群), Dan-Dan Liu(刘丹丹), Xiang-Dong Yang(杨向东)
Chin. Phys. B . 2016, 25(12): 126103. **doi:** 10.1088/1674-1056/25/12/126103

Theoretical calculations of structural, electronic, and elastic properties of $CdSe_{1-x}Te_x$: A first principles study

M Shakil, Muhammad Zafar, Shabbir Ahmed, Muhammad Raza-ur-rehman Hashmi, M A Choudhary, T Iqbal
Chin. Phys. B . 2016, 25(7): 076104. **doi:** 10.1088/1674-1056/25/7/076104

Confinement-induced modulation of elastic properties of nano-confined fluids in slit pore*

Zong-Li Sun(孙宗利)[1,†], Yan-Shuang Kang(康艳霜)[2,‡], and Yan-Mei Kang(康艳梅)[3]

[1] *Science and Technology College, North China Electric Power University, Baoding* 071051, *China*
[2] *College of Science, Hebei Agricultural University, Baoding* 071001, *China*
[3] *University of International Relations, Beijing* 100091, *China*

(Received 29 October 2018; revised manuscript received 16 January 2019; published online 22 February 2019)

Based on statistical mechanics for classical fluids, the general expressions for the elastic moduli of inhomogeneous fluid are derived and expressed as functionals of density functions. Within the framework of classical density functional theory, the bulk modulus of confined argon in slit pore is calculated under different conditions. The effects of vapor pressure, temperature, and pore width on modulus are calculated and investigated. Obvious confinement-induced effect has been observed in the confined argon. In addition, the solvation pressure dependence of the bulk modulus is also investigated, and the results suggest that the Tait–Murnaghan equation is still valid for the confined fluids.

Keywords: elastic modulus, confinement-induced modulation, confined argon, density functional

PACS: 61.20.Gy, 62.10.+s **DOI:** 10.1088/1674-1056/28/3/036102

1. Introduction

Recently, confinement-induced modulation in structural and thermodynamic properties of confined fluids has attracted considerable attention, due largely to the development of novel nanotechnological applications and advanced function materials.[1–3] In the nano-confined fluids, it has been found that the confinement can usually result in many novel thermodynamic phenomena, including phase transition,[4,5] thin-thick transition,[6] particle selectivity and exclusion,[7] etc. Besides, the thermodynamic and transport properties of nano-confined fluid, such as pressure,[8–10] elastics,[11,12] viscosity,[13,14] self-diffusion,[15,16] and thermal conductivity,[17,18] have also been found to be markedly different from those of bulk fluids. Actually, these properties can be modulated by the characteristics of the pore, including its dimension and strength. Among these properties, elastic modulus has an unique importance because it contains rich mechanics information, which is indispensable for description of the mechanical behaviors of materials.

To our best knowledge, the first study on the elastic property of confined fluids was conducted by Page *et al.*,[19] who applied the ultrasonic measurement to the n-hexane in Vycor glass. Recently, the method of ultrasonic measurement has also been employed, by Schappert *et al.*, to study the elastic modulus of argon,[20–22] nitrogen,[23] oxygen,[24] n-heptane, and n-nonane[25] in nano-pores, especially its vapor pressure dependence in both adsorption and desorption processes. In addition to the ultrasonic measurement, computer simulation is another efficient method, which has provided us with fruitful information about the elastic properties of the confined fluids. By performing grand canonical Monte Carlo (GCMC) simulation for confined argon in nano-pore, Gor *et al.* has studied the dependence of its isothermal bulk modulus on the pore size,[26] vapor pressure,[27] and pore geometry.[28] However, in either ultrasonic measurement or computer simulation, the modulus of the confined fluids has been regarded as a whole, which indicates that these studies have ignored the inhomogeneity and anisotropy of the elastic modulus.

Despite the success achieved in either ultrasonic measurement or computer simulation, both methods are too time-consuming. In order to obtain more comprehensive information about the modulus of confined fluids, it is expected that one can establish the relationship between modulus and microscopic structure of the system. Actually, when the liquid is experiencing a high frequency external force, it usually exhibits elastic behavior, just as the solid does. However, it is difficult to define the strain tensor in liquids due to the thermal motion and disorder of the liquid particles. To get around this problem, Schofield suggested that one can project the rate of stress fluctuation on the rate of strain.[29] Besides, Fisher[30] assumed that one can regard the liquid as a frozen solid, which has the same pair distribution function as that of the liquid under consideration. In this work, we employ the method of Fisher to derive general expressions for the elastic moduli, which is applicable to the confined fluids.

In statistical mechanics, most thermodynamic properties

*Project supported by the National Natural Science Foundation of China (Grant No. 21503077), the Fundamental Research Fund for the Central Universities of China (Grant No. 2016MS156), and the Research Project from Hebei Education Department, China (Grant No. QN2018119).

†Corresponding author. E-mail: sunzl@ncepu.edu.cn
‡Corresponding author. E-mail: kang_yanshuang@163.com

© 2019 Chinese Physical Society and IOP Publishing Ltd

of fluids can be expressed as functional of the density of particle. Then, numerical solution of equilibrium density has the primary necessity in the investigation. Actually, classical density functional theory (DFT) is a powerful tool for the description of classical many-particles system.[31,32] It has shown satisfactory performance in studies of various material phenomena for both atomic and colloidal systems. However, the lack of knowledge about the exact expression for the excess Helmholtz free energy requires approximation for it. Among all of the available approximations, the modified fundamental measure theory (MFMT) for hard sphere interaction[33] and weighted density approximation (WDA) for long-ranged attraction[34,35] have become the most preferred methods in the theoretical investigation on classical fluids.

Very recently, it is found that the pore geometry can influence the modulus of the confined fluids.[28] However, most of the existing reports focus mainly on the pores with spherical or cylindrical symmetry. Therefore, in this work, we aim to investigate the elastic modulus of confined fluids in slit pores. The paper is organized as follow. In Section 2, the general expressions of elastics moduli for inhomogeneous fluids are derived based on Hooke's law. In Section 3, the excess Helmholtz energy of Lennard–Jones (LJ) fluids is constructed by using of the Kolafa's equation of state. In Section 4, the elastic modulus for LJ fluid is calculated. In order to avoid the divergency of its hard sphere contribution, both moduli are related to the pressure and internal energy of the fluid. In Section 5, the effect of vapor pressure, temperature, and pore width on the bulk modulus of confined argon is calculated and studied. A conclusion is drawn in the last section.

2. Local elastic properties in the inhomogeneous fluids

It is well known that in the bulk case, the elastic moduli of the fluid are usually uniform. In contrast, for the confined fluid, it becomes position-dependent and anisotropic. Actually, in either bulk or confined fluid, one can always relate its elastic modulus to the change of the stress tensor through

$$\tilde{\boldsymbol{\Pi}} - \boldsymbol{\Pi} = \mu_T(\boldsymbol{T}_{\alpha\beta} + \boldsymbol{T}_{\beta\alpha}) + \left(K_T - \frac{2}{3}\mu_T\right)\boldsymbol{T}_{\alpha\alpha}. \tag{1}$$

This is exactly the Hooke's law.[36] Here, $\tilde{\boldsymbol{\Pi}}$ and $\boldsymbol{\Pi}$ are respectively the stress tensor after and before the deformation, while K_T and μ_T are respectively the isothermal bulk and shear moduli. In Eq. (1), $\boldsymbol{T}_{\alpha\beta}$ is the component of the strain tensor, which can be determined following the proposal by Fisher.[30]

In this work, the stress tensor, which is necessary in the calculation of the moduli, is given by the Irving–Kirkwood's expression[37]

$$\boldsymbol{\Pi} = -k_{\mathrm{B}}T\rho(\boldsymbol{r})\boldsymbol{I} + \frac{1}{2}\int \mathrm{d}\boldsymbol{r}_{12}\frac{\boldsymbol{r}_{12}\boldsymbol{r}_{12}}{r_{12}}\varphi'(r_{12}) \times \int_0^1 \mathrm{d}\xi\rho^{(2)}(\boldsymbol{r}-\xi\boldsymbol{r}_{12}, \boldsymbol{r}-\xi\boldsymbol{r}_{12}+\boldsymbol{r}_{12}), \tag{2}$$

where $\rho(\boldsymbol{r})$ and $\rho^{(2)}(\boldsymbol{r}_1,\boldsymbol{r}_2)$ are respectively the singlet and pair density functions, and $\boldsymbol{I}$ is unit tensor. In addition, k_{B} and T are Boltzmann constant and absolute temperature, respectively. $\xi \in (0,1)$ is a constant and $\varphi(r_{12})$ is the pair potential with $r_{12} = |\boldsymbol{r}_{12}|$ and $\boldsymbol{r}_{12} = \boldsymbol{r}_2 - \boldsymbol{r}_1$. On the right hand of Eq. (2), the first and second terms denote respectively the kinetic and interaction contributions. Actually, the kinetic contribution of the moduli can be exactly given by $K_T^{\mathrm{id}} = \frac{5}{3}k_{\mathrm{B}}T\rho$ and $\mu_T^{\mathrm{id}} = k_{\mathrm{B}}T\rho$. Therefore, in the following, we focus only on the interaction contribution of the moduli.

When the fluid experiences a deformation, the interaction contribution after the deformation can also be given in terms of the Irving–Kirkwood expression

$$\tilde{\boldsymbol{\Pi}}^{\mathrm{int}} = \frac{1}{2}\int \mathrm{d}\tilde{\boldsymbol{r}}_{12}\frac{\tilde{\boldsymbol{r}}_{12}\tilde{\boldsymbol{r}}_{12}}{\tilde{r}_{12}}\varphi'(\tilde{r}_{12}) \times \int_0^1 \mathrm{d}\xi\tilde{\rho}^{(2)}(\tilde{\boldsymbol{r}}-\xi\tilde{\boldsymbol{r}}_{12}, \tilde{\boldsymbol{r}}-\xi\tilde{\boldsymbol{r}}_{12}+\tilde{\boldsymbol{r}}_{12}). \tag{3}$$

Note that in Eq. (3) and hereafter, tildes have been used to distinguish the qualities after deformation from those before deformation. Further, it is assumed that during the deformation, the particle at $\boldsymbol{r}_1$ experiences a displacement $\boldsymbol{t}$, which satisfies

$$\tilde{\boldsymbol{r}}_1 = \boldsymbol{r}_1 + \boldsymbol{t}(\boldsymbol{r}_1). \tag{4}$$

Similarly, another position vector $\boldsymbol{r}_2$, which has a distance $\boldsymbol{r}_{12} \equiv \boldsymbol{r}_2 - \boldsymbol{r}_1$ from $\boldsymbol{r}_1$, changes to

$$\tilde{\boldsymbol{r}}_2 = \boldsymbol{r}_2 + \boldsymbol{t}(\boldsymbol{r}_1 + \boldsymbol{r}_{12}). \tag{5}$$

Combining the above two equations, the distance between the two positions after deformation can be given by

$$\tilde{\boldsymbol{r}}_{12} = \tilde{\boldsymbol{r}}_2 - \tilde{\boldsymbol{r}}_1 = \boldsymbol{r}_{12} + \boldsymbol{r}_{12}\cdot\boldsymbol{T}(\boldsymbol{r}_1), \tag{6}$$

with the strain tensor $\boldsymbol{T}(\boldsymbol{r}) = \boldsymbol{\nabla}\boldsymbol{t}(\boldsymbol{r})$. According to the above equations, one can easily obtain the ratio of volume elements after and before the deformation

$$\frac{\mathrm{d}\tilde{\boldsymbol{r}}_i}{\mathrm{d}\boldsymbol{r}_i} = \frac{\mathrm{d}\tilde{\boldsymbol{r}}_{ij}}{\mathrm{d}\boldsymbol{r}_{ij}} = 1 + \sum_\alpha T_{\alpha\alpha}. \tag{7}$$

Here, it is necessary to note that the superscripts $i, j = 1, 2$ are used to distinguish the particles, and that $T_{\alpha\alpha}$ denotes the magnitude of the diagonal element of $\boldsymbol{T}$.

During the deformation, the particle number in a selected volume should keep unchanged, which indicates that $\tilde{\rho}(\tilde{\boldsymbol{r}}_1)\mathrm{d}\tilde{\boldsymbol{r}}_1 = \rho(\boldsymbol{r}_1)\mathrm{d}\boldsymbol{r}_1$. Accordingly, one can obtain the relationship between the densities after and before the deformation

$$\tilde{\rho}(\tilde{\boldsymbol{r}}_1) = \frac{\rho(\boldsymbol{r}_1)}{1 + \sum_\alpha T_{\alpha\alpha}}. \tag{8}$$

By the same reason, the probability of simultaneously finding particle 1 in $\mathrm{d}\boldsymbol{r}_1$ and particle 2 in $\mathrm{d}\boldsymbol{r}_2$ in the initial system

should also be equal to that of simultaneously finding particle 1 in $\mathrm{d}\tilde{\boldsymbol{r}}_1$ and particle 2 in $\mathrm{d}\tilde{\boldsymbol{r}}_2$ in the deformed system, that is, $\tilde{\rho}^{(2)}(\tilde{\boldsymbol{r}}_1,\tilde{\boldsymbol{r}}_2)\mathrm{d}\tilde{\boldsymbol{r}}_1\mathrm{d}\tilde{\boldsymbol{r}}_2=\rho^{(2)}(\boldsymbol{r}_1,\boldsymbol{r}_2)\mathrm{d}\boldsymbol{r}_1\mathrm{d}\boldsymbol{r}_2$. Thence,

$$\tilde{\rho}^{(2)}(\tilde{\boldsymbol{r}}_1,\tilde{\boldsymbol{r}}_2)=\frac{\rho^{(2)}(\boldsymbol{r}_1,\boldsymbol{r}_2)}{(1+\sum_\alpha T_{\alpha\alpha})^2}. \tag{9}$$

Based on Eqs. (7) and (9), one can obtain the relationship

$$\frac{\tilde{\rho}^{(2)}(\tilde{\boldsymbol{r}}-\xi\tilde{\boldsymbol{r}}_{12},\tilde{\boldsymbol{r}}-\xi\tilde{\boldsymbol{r}}_{12}+\tilde{\boldsymbol{r}}_{12})\mathrm{d}\tilde{\boldsymbol{r}}_{12}}{\rho^{(2)}(\boldsymbol{r}-\xi\boldsymbol{r}_{12},\boldsymbol{r}-\xi\boldsymbol{r}_{12}+\boldsymbol{r}_{12})\mathrm{d}\boldsymbol{r}_{12}}\simeq 1-\sum_\alpha T_{\alpha\alpha}, \tag{10}$$

because it has been assumed that the deformation is small, as the Hooke's law requires. To relate other qualities of the deformed system with those of the initial system, we perform Taylor expansion on them around the corresponding qualities of initial system. In these expansions, only the linear terms of the strain tensor are retained because of the requirement of the Hooke's law. Therefore, we obtain

$$\begin{aligned}\tilde{\boldsymbol{r}}_{12}\tilde{\boldsymbol{r}}_{12} &= [\boldsymbol{r}_{12}+\boldsymbol{r}_{12}\cdot\boldsymbol{T}][\boldsymbol{r}_{12}+\boldsymbol{r}_{12}\cdot\boldsymbol{T}]\\ &= \boldsymbol{r}_{12}\boldsymbol{r}_{12}+x_\alpha x_\beta(\boldsymbol{T}_{\alpha\beta}+\boldsymbol{T}_{\beta\alpha}),\end{aligned} \tag{11}$$

where x_α is the Cartesian component of $\boldsymbol{r}_{12}$, and

$$\frac{\varphi'(\tilde{r}_{12})}{\tilde{r}_{12}}=\frac{\varphi'(r_{12})}{r_{12}}+\frac{\mathrm{d}}{\mathrm{d}r_{12}}\left[\frac{\varphi'(r_{12})}{r_{12}}\right]\frac{\boldsymbol{r}_{12}}{r_{12}}\cdot(\boldsymbol{r}_{12}\cdot\boldsymbol{T}). \tag{12}$$

Inserting Eqs. (7)–(12) into Eq. (3), and after some simple but tedious algebraic operations, one can obtain the change of stress during the deformation as

$$\begin{aligned}&\tilde{\boldsymbol{\Pi}}^{\mathrm{int}}-\boldsymbol{\Pi}^{\mathrm{int}}\\ &=-\frac{1}{2}\left(\sum_\alpha T_{\alpha\alpha}\right)\int\mathrm{d}\boldsymbol{r}_{12}\frac{\boldsymbol{r}_{12}\boldsymbol{r}_{12}}{r_{12}}\varphi'(r_{12})\\ &\quad\times\int_0^1\mathrm{d}\xi\rho^{(2)}(\boldsymbol{r}-\xi\boldsymbol{r}_{12},\boldsymbol{r}-\xi\boldsymbol{r}_{12}+\boldsymbol{r}_{12})\\ &\quad+\frac{1}{2}\int\mathrm{d}\boldsymbol{r}_{12}\frac{\varphi'(r_{12})}{r_{12}}\left[x_\alpha x_\beta\left(\boldsymbol{T}_{\alpha\beta}+\boldsymbol{T}_{\beta\alpha}\right)\right]\\ &\quad\times\int_0^1\mathrm{d}\xi\rho^{(2)}(\boldsymbol{r}-\xi\boldsymbol{r}_{12},\boldsymbol{r}-\xi\boldsymbol{r}_{12}+\boldsymbol{r}_{12})\\ &\quad+\frac{1}{2}\int\mathrm{d}\boldsymbol{r}_{12}\frac{\mathrm{d}}{\mathrm{d}r_{12}}\left[\frac{\varphi'(r_{12})}{r_{12}}\right]\frac{1}{r_{12}}(\boldsymbol{r}_{12}\boldsymbol{r}_{12}\boldsymbol{r}_{12}\boldsymbol{r}_{12}:\boldsymbol{T})\\ &\quad\times\int_0^1\mathrm{d}\xi\rho^{(2)}(\boldsymbol{r}-\xi\boldsymbol{r}_{12},\boldsymbol{r}-\xi\boldsymbol{r}_{12}+\boldsymbol{r}_{12}).\end{aligned} \tag{13}$$

Taking into account the fact that

$$\int\mathrm{d}\boldsymbol{r}_{12}x_\alpha x_\beta f(r_{12})=\frac{1}{3}\int\mathrm{d}\boldsymbol{r}_{12}r_{12}^2f(r_{12})\boldsymbol{I} \tag{14}$$

and that

$$\begin{aligned}&\int\mathrm{d}\boldsymbol{r}_{12}(\boldsymbol{r}_{12}\boldsymbol{r}_{12}\boldsymbol{r}_{12}\boldsymbol{r}_{12}:\boldsymbol{T})f(r_{12})\\ &=\frac{1}{15}\int\mathrm{d}\boldsymbol{r}_{12}r_{12}^4f(r_{12})\left(\sum_\alpha T_{\alpha\alpha}\boldsymbol{I}+\boldsymbol{T}_{\alpha\beta}+\boldsymbol{T}_{\beta\alpha}\right),\end{aligned} \tag{15}$$

the change of the stress tensor during the deformation can be rewritten as

$$\begin{aligned}&\tilde{\boldsymbol{\Pi}}^{\mathrm{int}}-\boldsymbol{\Pi}^{\mathrm{int}}\\ &=-\frac{I_1(\boldsymbol{r})}{6}\left(\sum_\alpha T_{\alpha\alpha}\boldsymbol{I}\right)+\frac{I_1(\boldsymbol{r})}{6}\left(\boldsymbol{T}_{\alpha\beta}+\boldsymbol{T}_{\beta\alpha}\right)\\ &\quad+\frac{I_2(\boldsymbol{r})-I_1(\boldsymbol{r})}{30}\left(\sum_\alpha T_{\alpha\alpha}\boldsymbol{I}+\boldsymbol{T}_{\alpha\beta}+\boldsymbol{T}_{\beta\alpha}\right).\end{aligned} \tag{16}$$

In the above equation, two auxiliary integrals I_1 and I_2 have been respectively defined as

$$\begin{aligned}I_1(\boldsymbol{r}) &= \frac{1}{2}\int\mathrm{d}\boldsymbol{r}_{12}r_{12}\varphi'(r_{12})\\ &\quad\times\int_0^1\mathrm{d}\xi\rho^{(2)}(\boldsymbol{r}-\xi\boldsymbol{r}_{12},\boldsymbol{r}-\xi\boldsymbol{r}_{12}+\boldsymbol{r}_{12})\end{aligned} \tag{17}$$

and

$$\begin{aligned}I_2(\boldsymbol{r}) &= \frac{1}{2}\int\mathrm{d}\boldsymbol{r}_{12}r_{12}^2\varphi''(r_{12})\\ &\quad\times\int_0^1\mathrm{d}\xi\rho^{(2)}(\boldsymbol{r}-\xi\boldsymbol{r}_{12},\boldsymbol{r}-\xi\boldsymbol{r}_{12}+\boldsymbol{r}_{12}).\end{aligned} \tag{18}$$

By comparing Eq. (16) with Eq. (1), we obtain the expressions for the isothermal shear and bulk modulus as

$$\mu_T(\boldsymbol{r})=k_{\mathrm{B}}T\rho(\boldsymbol{r})+\frac{4}{15}I_1(\boldsymbol{r})+\frac{1}{15}I_2(\boldsymbol{r}), \tag{19}$$

$$K_T(\boldsymbol{r})=\frac{5}{3}k_{\mathrm{B}}T\rho(\boldsymbol{r})-\frac{2}{9}I_1(\boldsymbol{r})+\frac{1}{9}I_2(\boldsymbol{r}). \tag{20}$$

These two equations are the main theoretical results of this work. Obviously, it can reduce to the results of Schofield, whose calculation is based on the thermodynamic fluctuation theory.[29] However, it is more applicable for the description of the elastic properties of the confined fluid, because the involved inhomogeneous pair density function $\rho^{(2)}(\boldsymbol{r}-\xi\boldsymbol{r}_{12},\boldsymbol{r}-\xi\boldsymbol{r}_{12}+\boldsymbol{r}_{12})$ contains more correlation information than the radial distribution function alone.

3. Free energy functional for the inhomogeneous Lennard–Jones fluid

In this work, we focus on the elastic properties of confined Lennard–Jones fluid, in which the inter-particle interaction can be described by the pair potential

$$\varphi(r)=4\varepsilon\left[\left(\frac{\sigma}{r}\right)^{12}-\left(\frac{\sigma}{r}\right)^{6}\right], \tag{21}$$

where ε and σ stand respectively for the size and energy parameters of the LJ potential. In the Barker–Henderson scheme,[38] the LJ potential can be decomposed into hard sphere and attractive contributions. That is,

$$\varphi(r)=\varphi_{\mathrm{hs}}(r)+\varphi_{\mathrm{att}}(r), \tag{22}$$

where

$$\varphi_{\mathrm{hs}}(r)=\begin{cases}\infty, & r<d,\\ 0, & d<r,\end{cases} \tag{23}$$

$$\varphi_{\rm att}(r)=\begin{cases}0, & r<\sigma,\\ \varphi(r), & \sigma<r<r_{\rm c},\\ 0, & r_{\rm c}<r.\end{cases} \tag{24}$$

Here, d is the effective hard sphere diameter, while $r_{\rm c}$ is the cut-off of the LJ potential.

Based on such decomposition of the pair potential, the Helmholtz free energy of the LJ fluids can be expressed as

$$F[\rho(\boldsymbol{r})]=F_{\rm id}[\rho(\boldsymbol{r})]+F_{\rm hs}[\rho(\boldsymbol{r})]+F_{\rm att}[\rho(\boldsymbol{r})], \tag{25}$$

where $F_{\rm id}=k_{\rm B}T\int\rho(\boldsymbol{r})\{\ln[\rho(\boldsymbol{r})\Lambda^3]-1\}{\rm d}\boldsymbol{r}$ is exactly known. In addition, the hard sphere contribution $F_{\rm hs}[\rho(\boldsymbol{r})]$ can be given by MFMT, which is proposed by Yu *et al.*[33] In the MFMT, the hard sphere contribution is expressed as

$$F_{\rm hs}[\rho(\boldsymbol{r})]=k_{\rm B}T\int\Phi_{\rm hs}[n_\alpha]{\rm d}\boldsymbol{r}, \tag{26}$$

where $\Phi_{\rm hs}$ is the reduced excess Helmholtz free-energy density and n_α is the related weighted densities. Note that for the LJ fluid, its effective hard sphere diameter d can be given by[39]

$$d=\frac{1+0.2977T^*}{1+0.33163T^*+0.0010477T^{*2}}\sigma, \tag{27}$$

where $T^*=k_{\rm B}T/\varepsilon$ is the reduced temperature. The details about the calculation of the weighted density can be found in the literature.[33]

In the treatment of the attractive contribution, say $F_{\rm att}[\rho(\boldsymbol{r})]$, weighted density approximation has been found to be an efficient method. In WDA for attraction contribution, the Helmholtz free energy can be obtained from the equation of state for bulk phase, by replacing the bulk density with a weighted density $\bar{\rho}(\boldsymbol{r})$, which is given by

$$\bar{\rho}(\boldsymbol{r})=\int\rho(\boldsymbol{r}')\omega(|\boldsymbol{r}'-\boldsymbol{r}|){\rm d}\boldsymbol{r}'. \tag{28}$$

Here, the weight function $\omega(r)=\frac{3}{4\pi d^3}\Theta(r-d)$ is a preferred choice in the calculation. Among the existing equations of state for the LJ fluid, we employ the one proposed by Kolafa *et al.*, who expressed the contribution from the attraction in the following form:[40]

$$\begin{aligned}F_{\rm att} &= \rho^*(1-2\gamma\rho^{*2})\exp(-\gamma\rho^{*2})\Delta B_{2,\rm hBH}\\ &\quad+\sum_{ij}jC_{ij}T^{*\frac{i}{2}-1}\rho^{*j},\end{aligned} \tag{29}$$

where $\rho^*=\rho d^3$ is the reduced density. The definition of the coefficients γ, $\Delta B_{2,\rm hBH}$, and C_{ij} in Eq(29) can be found in the literature.[40]

4. Elastic moduli of the inhomogeneous Lennard–Jones fluid in confinement

In the above section, we have derived the expressions for the bulk and shear moduli with the aid of two auxiliary integrals I_1 and I_2, which are given in Eqs. (17) and (18), respectively. Actually, both integrals can be rewritten in the following compact form:

$$\begin{aligned}I_m(\boldsymbol{r}) &= \frac{1}{2}\int{\rm d}\boldsymbol{r}_{12}r_{12}^m\varphi^{(m)}(r_{12})\\ &\quad\times\int_0^1{\rm d}\xi\rho^{(2)}(\boldsymbol{r}-\xi\boldsymbol{r}_{12},\boldsymbol{r}-\xi\boldsymbol{r}_{12}+\boldsymbol{r}_{12}),\end{aligned} \tag{30}$$

where $m=1,2$ correspond to I_1 and I_2, respectively. Here, $\varphi^{(m)}(r_{12})$ is the m-th order derivative of the pair potential with respect to r_{12}.

According to the decomposition of $\varphi(r)$ in Eq. (22), the above two integrals should also be regarded as the sum of hard sphere and attraction contributions, that is,

$$I_m(\boldsymbol{r})=I_m^{\rm hs}(\boldsymbol{r})+I_m^{\rm att}(\boldsymbol{r}). \tag{31}$$

Actually, the calculation of $I_m^{\rm att}(\boldsymbol{r})$ is convenient because the long-ranged attractive tail is analytic in the whole region. In addition, $I_1^{\rm hs}(\boldsymbol{r})$ can also be determined due to the fact that $\varphi'_{\rm hs}(r)=-k_{\rm B}T\delta(r-d)$. In contrast, the calculation of $I_2^{\rm hs}(\boldsymbol{r})$, which involves $\varphi''_{\rm hs}(r)$, is unfulfillable by performing direct integration, because it usually gives infinite result, as shown by Heyes *et al.*[41] Therefore, the integral I_1 can be calculated directly by the integration in Eq. (30), while I_2 fails.

As an alternative method for the calculation of I_2, we employ the one proposed by Zwanzig *et al.*,[42] who expressed the shear modulus through the pressure and internal energy of the LJ system. In the bulk phase of an LJ system, the pressure and internal energy contributed from one particle can be respectively given by

$$P=k_{\rm B}T\rho_{\rm b}-\frac{1}{6}\rho_{\rm b}^2\int{\rm d}\boldsymbol{r}_{12}r_{12}\varphi'(r_{12})g(r_{12}), \tag{32}$$

$$E=\frac{3}{2}k_{\rm B}T-\frac{1}{2}\rho_{\rm b}\int{\rm d}\boldsymbol{r}_{12}\varphi(r_{12})g(r_{12}). \tag{33}$$

Substituting the pair potential, say $\varphi(r)$, into Eqs. (20), (32), and (33), one can obtain I_2 for the bulk LJ system

$$I_2^{\rm b}=51k_{\rm B}T\rho_{\rm b}+57P-72\rho_{\rm b}E. \tag{34}$$

Adopting the idea of WDA, one can replace the bulk density $\rho_{\rm b}$ with the weighted density $\bar{\rho}(\boldsymbol{r})$. Therefore, equation (34) provides us with an effective treatment for the calculation of $I_2(\boldsymbol{r})$ for the inhomogeneous LJ fluid. In this work, the expressions for both P and E are given by equation of state proposed by Kolafa *et al.*,[40] that is,

$$\begin{aligned}P^* &= \rho^*T^*z_{\rm hs}+\rho^{*2}T^*(1-2\gamma\rho^{*2})\exp(-\gamma\rho^{*2})\Delta B_{2,\rm hBH}\\ &\quad+\rho^{*2}T^*\sum_{ij}jC_{ij}T^{*\frac{i}{2}-1}\rho^{*j},\end{aligned} \tag{35}$$

where $P^* = P\frac{\sigma^3}{\varepsilon}$, $z_{\rm hs} = \frac{1+\eta+\eta^2-\frac{2}{3}\eta^3(1+\eta)}{(1-\eta)^3}$, and $\eta = \frac{\pi}{6}\rho d^3$. In the same level, the internal energy contributed from one particle is

$$E^* = \frac{3(z_{\rm hs}-1)}{d_{\rm hBH}}\frac{\partial d_{\rm hBH}}{\partial(1/T^*)} + \rho^* \exp(-\gamma\rho^{*2})\frac{\partial \Delta B_{2,\rm hBH}}{\partial(1/T^*)} - \sum_{ij}\left(\frac{i}{2}-1\right)C_{ij}T^{*\frac{i}{2}}\rho^{*j}, \quad (36)$$

where $E^* = E/\varepsilon$, and $d_{\rm hBH}$ is the effective hard sphere diameter.[40]

5. Results and discussion

In this work, we assume that the LJ fluid is confined in a slit pore. For such an inhomogeneous system, the elastic properties should also exhibit position-dependence, which arises from the inhomogeneous density profile and the close relation between moduli and fluid structure. Actually, equations (19) and (20) suggest that the density profile is one critical factor in determining the elastic properties of the confined fluid. Therefore, prior to the calculation of the moduli, one should firstly calculate the equilibrium density of the fluid in the pore.

In order to test the performance of the free energy functional that has been constructed for the DFT calculation, we have calculated the density profiles of the LJ fluids confined in the slit pores, whose external potential is described by the Steele 10-4-3 potential.[43] In the calculation, the pore widths are set as $H/\sigma = 2.0$, 4.0, and 7.5, the bulk density $\rho_{\rm b}\sigma^3 = 0.5925$, and the reduced temperature $T^* = 1.2$. The results depicted in Fig. 1 suggest that our results of the density profiles, for all of the chosen pore widths, agree very well with those from the grand canonical ensemble Monte Carlo simulations.[44]

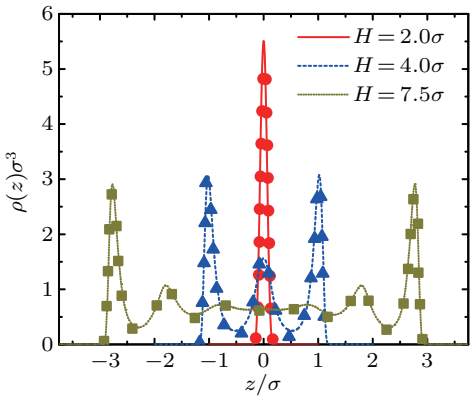


Fig. 1. The equilibrium density profiles of LJ fluids that confined in slit pores. In the calculations, the input parameters are set as $H/\sigma = 2.0$, 4.0, and 7.5, $\rho_{\rm b}\sigma^3 = 0.5925$, and $T^* = 1.2$. The symbols are the results from the GCMC simulations.[44]

To further validate the effectiveness of the theoretical results that have been obtained in the above section, we have also calculated the bulk modulus of the confined argon in a spherical pore. The parameters used in our calculation are set the same as those in the GCMC simulation, which is carried out, by Gor *et al.*,[28] for the confined argon. Note that in their simulation, the elastic property of the confined system is regarded as a whole. Therefore, for the comparison purpose, we have calculated the spatial average of the inhomogeneous bulk modulus in the pores

$$\overline{K}_T = \frac{2}{D}\int_0^{D/2} K_T(r)\mathrm{d}r, \quad (37)$$

where D is the diameter of the pore. In Fig. 2, our results are compared with those obtained by the GCMC simulation for the same systems. The results for $D = 3$ nm, 4 nm, and 5 nm suggest that our derivation can describe the elastic properties of confined fluid very well.

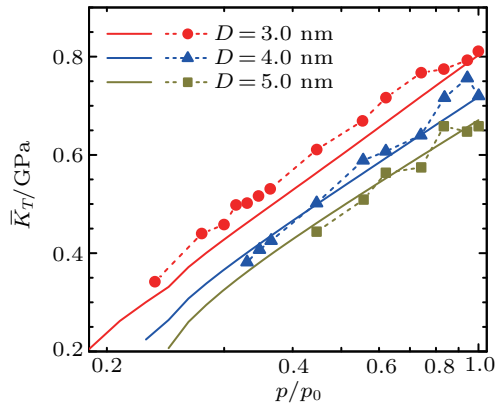


Fig. 2. The averaged isothermal bulk modulus of argon that confined in spherical pores with diameters $D = 3$ nm, 4 nm, and 5 nm. The solid lines are the results based on our theoretical derivation, while the symbols stand for the results from GCMC simulations.[28] Note that the dashed lines are plotted only to guide eyes.

In the following sections, we focus on the confinement-induced modulation of the isothermal bulk modulus of argon, which is confined in a slit pore. The external potential exerted on the particles by the pore can be given by

$$V_{\rm ext}(z) = 2\pi\rho_{\rm s}\varepsilon_{\rm fs}\sigma_{\rm fs}^2\left\{\frac{2}{5}\left[\left(\frac{\sigma_{\rm fs}}{z}\right)^{10} + \left(\frac{\sigma_{\rm fs}}{H-z}\right)^{10}\right] - \left[\left(\frac{\sigma_{\rm fs}}{z}\right)^{4} + \left(\frac{\sigma_{\rm fs}}{H-z}\right)^{4}\right]\right\}, \quad (38)$$

where H is the pore width and z is the distance of particle apart from the left wall. In our calculation, the input parameters for the pore are set as:[28] solid atom density $\rho_{\rm s} = 15.3\ {\rm nm}^{-2}$, wall strength $\varepsilon_{\rm fs}/k_{\rm B} = 171.24$ K, and the solid–fluid collision diameter $\sigma_{\rm fs} = 0.3$ nm. In addition, input parameters for argon are set as: $\sigma = 0.3405$ nm, $\varepsilon/k_{\rm B} = 119.6$ K, and the cut off radius $r_{\rm c} = 5\sigma$.

5.1. Local profile of the bulk modulus in confined argon

As stated in the above section, the modulus of the confined fluid should be position-dependent because of its close relation with the inhomogeneous density. From a microscopic

point of view, the inhomogeneous modulus arises from the interaction between the particles. Specifically, the hard sphere repulsion usually leads to the enhancement of the modulus, as it tends to prevent the fluid from being compressed because of the excluded volume effect. Therefore, the profiles of the modulus in the pore exhibit oscillation, as shown in Figs. 3(a) and 3(b). In addition, the period of oscillation is nearly equal to the particle diameter, which indicates the importance of excluded volume in determining the modulus.

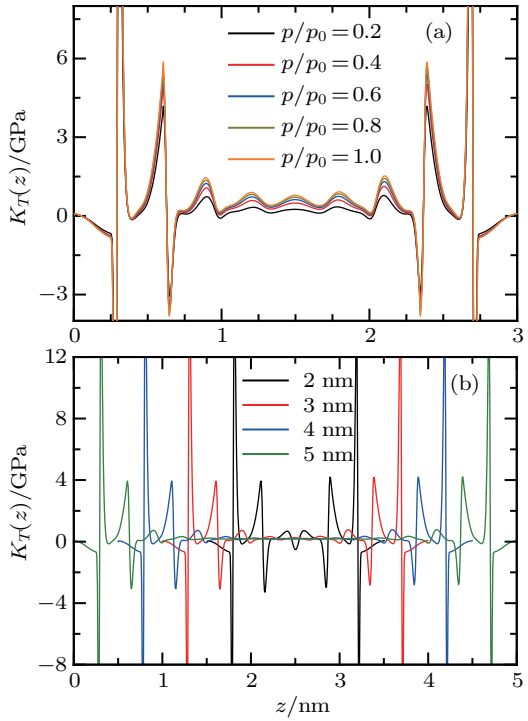


Fig. 3. The inhomogeneous profiles of isothermal bulk modulus, at $T = 87.3$ K, for argon confined in slit pore. (a) The pore width is set as $H = 3$ nm, and $p/p_0 = 0.2$, 0.4, 0.6, 0.8, and 1.0. (b) The vapor pressure is set as $p/p_0 = 0.2$, and $H = 2$ nm, 3 nm, 4 nm, and 5 nm.

Figure 3(a) depicts the influence of bulk pressure p_0 on the bulk modulus K_T in the slit pore. The results in it suggest that as p is increased, both the bulk modulus and the amplitude of its oscillation are enhanced. In addition, the notable change in its magnitude locates only in the central region. This can be explained by the occurrence of the capillary condensation. At the early stage of the condensation, the pore wall is covered by a multilayered film due to the adsorption, while in the middle region that is far from the wall, it keeps the vapor phase. As p approaches the saturated pressure p_0, the pore is full of condensed liquid phase, in which the layer structure is more obvious because the excluded volume grows stronger.

In Fig. 3(b), we have plotted the profiles of $K_T(z)$ for argon that is confined in pores with different width. The results show that the modulus near the wall is nearly equal for each of them, and that the difference between them locates only in the central region of the pore. In addition, in each curve for the modulus profile, there is a narrow region where the local modulus is negative. Actually, the negative modulus in confined fluids has been reported for different systems.[45,46] It has been found that the negative modulus always relates to the gas–liquid or liquid–solid transition, which can be stabilized by confinement. In fact, our results for the equilibrium density suggest that the negative modulus locates just right between two layers, where there is an obvious gas–liquid interface.

5.2. Effect of pressure and temperature on the bulk modulus in confined argon

In thermodynamics, state parameters, including p, V, and T, are critical factors in determining other thermodynamic properties. Among the above state parameters, p and T are intensive quantities, while V is an extensive quantity. In light of such a difference, it is expected that these two types of quantity may exert different effects on the elastic property of the confined fluid. In this section, we firstly investigate the influence of pressure on the bulk modulus for different pore widths. The calculation is carried out at two different temperatures, 87.3 K and 119.6 K, and the results are shown in Figs. 4(a) and 4(b), respectively.

In Fig. 4(a), it is found that for the case of $H = 2$ nm, $\overline{K}_T$ shows a logarithmic dependence on the relative pressure, while for $H > 2$ nm, a jump in the curves of $\overline{K}_T - p/p_0$ is observed before the appearance of the logarithmic dependence. This can be attributed to the occurrence of capillary condensation, which is obvious in the phase diagram shown in Fig. 4(c). Moreover, with the increase of the pore width, the jump point shifts towards the higher pressure. The logarithmic dependence of $\overline{K}_T$ on the relative pressure suggests that besides the bulk fluid, the elastic modulus of confined fluid also satisfies the Tait–Murnaghan equation,[47] which will be investigated in detail in Section 5.4. In addition, the results in Figs. 4(b) and 4(d) suggest that at a higher temperature, the capillary condensation is postponed because the attraction between particles is suppressed by the more violent thermal motion. This leads not only to a smaller magnitude of $\overline{K}_T$, but also to a larger jump point in the curves.

In Figs. 5(a)–5(c), the temperature dependence of $\overline{K}_T$ is calculated in the cases of different H and p/p_0 values. The results in Figs. 5(a) and 5(b) suggest that in the low temperature region, each $\overline{K}_T$–T curve shows a linear dependence with a constant slope. With the increase of T, however, $\overline{K}_T$ drops down to that of the bulk vapor phase. In addition, the drop point shifts to a lower temperature for the larger pore width. Actually, this arises from the advantage of the thermal motion over the inter-particle attraction in their competition, because in a pore with larger width, the particle is hard to condense across the pore. Our further calculation in Fig. 5(c) suggests that for a high enough p/p_0, the drop in $\overline{K}_T$ disappears in the whole temperature region, in which the calculation are performed.

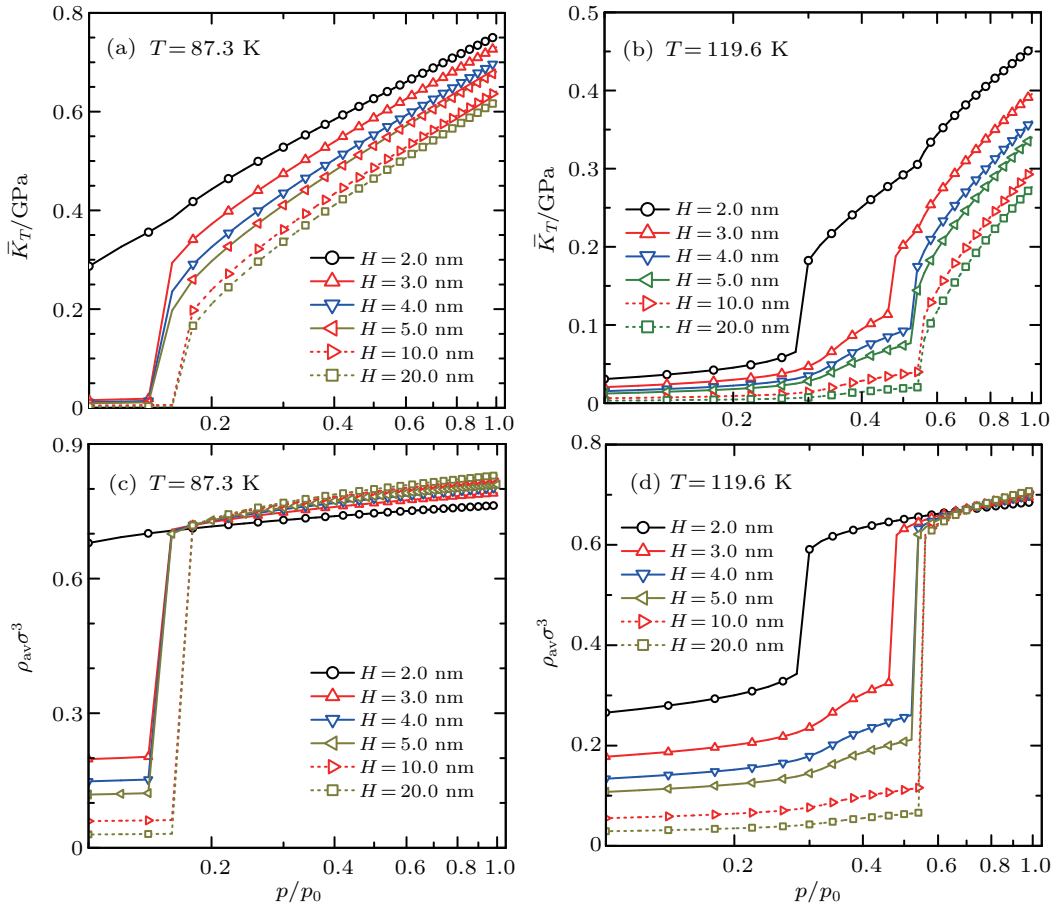


Fig. 4. (a) and (b) Pressure dependence of the spatial averaged isothermal bulk modulus under different conditions of pore width and temperature. (c) and (d) Phase diagrams for the confined argon under different conditions of pore width and temperature.

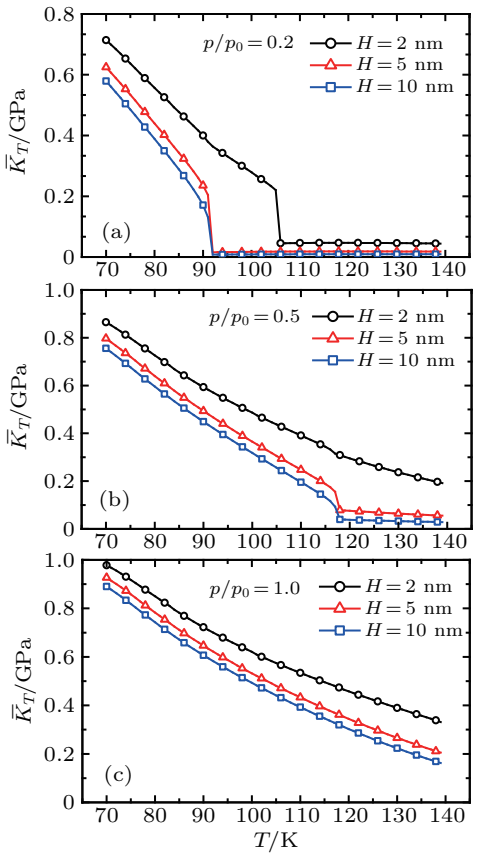


Fig. 5. The temperature dependence of the spatial averaged isothermal bulk modulus under different conditions of pore width and relative pressure.

5.3. Effect of pore width on the bulk modulus in confined argon

It is known that the pore width H relates to the volume of the system, which is an extensive quality. The investigation in the previous section reveals that the intensive qualities p and T influence $\overline{K}_T$ through their influence on the occurrence of capillary condensation in the pore. Here, we expect that the pore width H may exert different influence on $\overline{K}_T$. To this end, we have calculated the $\overline{K}_T$–H dependence under different conditions of p/p_0. The results for $T = 87.3$ K and 119.6 K are respectively given in Figs. 6(a) and 6(b).

In both figures, the results suggest that when H is small, the $\overline{K}_T$–H curves show obvious oscillation with the pore width. Moreover, the period of the oscillation is equal nearly to the particle diameter, which indicates again the importance of hard sphere contribution to the modulus. Actually, such a confinement-induced modulation can be understood as follows. When the pore is full with densely arranged layers, the system is hard to deform because of the strong excluded volume interaction between the adjacent layers. On the contrary, if there is space that is not occupied, the system can be easily deformed. Further, the results in both figures also suggest that when H is large enough, the oscillation in $\overline{K}_T$ disappears, and that it decreases gradually to the value of the corresponding

bulk vapor phase.

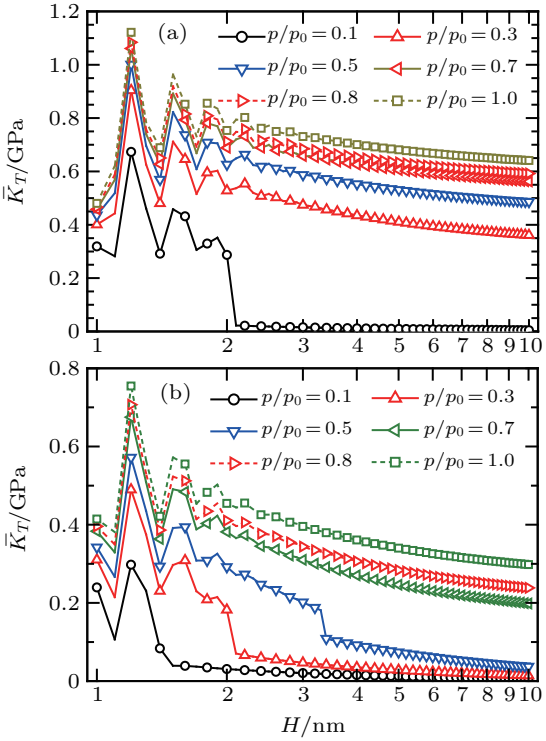


Fig. 6. The dependence of spatial averaged isothermal bulk modulus on the pore width under different conditions of relative pressure. The results in (a) and (b) correspond respectively to $T = 87.3$ K and 119.6 K.

5.4. Tait–Murnaghan equation for the confined argon in the slit pore

In the bulk fluids, the pressure dependence of bulk modulus can usually be linearly approximated by the Tait–Murnaghan equation[47]

$$\overline{K}_T(P) = \overline{K}_T^0 + \alpha(P - P_0), \tag{39}$$

where P is the solvation pressure and $\overline{K}_T^0$ is the modulus at some reference pressure P_0. The solvation pressure is even relevant because it plays an important role in determining the compressibility of the fluid. During the adsorption of argon in the pore, capillary condensation can usually take place even at the relative pressure $p/p_0 < 1$. The condensed fluid forms concave menisci at the pore entrances, and the negative solvation pressure at these menisci stretches the fluid. In such a case, the stretched fluid is much easier to be compressed than the fluid which is not stretched.

As shown by Gor *et al.*,[48,49] the solvation pressure in the capillary condensed fluid can be expressed as

$$P = -\frac{\gamma_{\rm sl}}{R} + \frac{R_{\rm g}T}{V_{\rm m}} \ln\left(\frac{p}{p_0}\right) + (p_0 - p), \tag{40}$$

where $\gamma_{\rm sl}$ is the solid–liquid surface tension, and R is the radius of the pore. Moreover, $R_{\rm g}$ and $V_{\rm m}$ are, respectively, the gas constant and mole volume of the fluid. Note that p_0–p is negligible compared with the other two contributions, and that for the given pore and type of fluid, $-\frac{\gamma_{\rm sl}}{R}$ keeps unchanged during the modulation of the relative pressure. Therefore, in this work, we focus only on the influence of the Laplace pressure, which can be given by the Kelvin–Laplace equation[27,48]

$$P_{\rm L} = \frac{R_{\rm g}T}{V_{\rm m}} \ln\left(\frac{p}{p_0}\right). \tag{41}$$

In Fig. 7, we have plotted the $\alpha - 1/H$ curve for the confined argon in the slit pore. The results for both $T = 87.3$ K and 119.6 K suggest that when H is small, the parameter α shows an oscillatory dependence on the pore width. Moreover, the period of the oscillation in the curve is nearly equal to the particle diameter. In contrast, when the pore width is large enough, α increases linearly with the decrease of $1/H$, and changes asymptotically to the value of the bulk fluid. Therefore, it can be concluded from our calculation that the Tait–Murnaghan equation is still valid for the confined fluids, while the parameter α can be significantly modulated by the confinement.

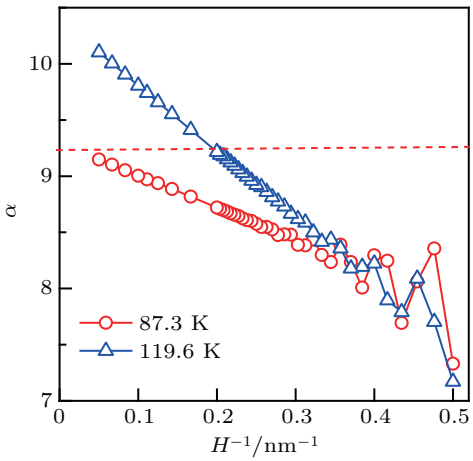


Fig. 7. The slope parameter α in the Tait–Murnaghan equation for the confined argon in slit pores with different widths. The dashed line in the figure represents the value of α for the corresponding bulk fluid at $T = 87.3$ K.

6. Conclusion

In this work, we have derived the general expressions for the bulk and shear moduli, which are written as functionals of the density functions. These results can return exactly to the bulk results which have been derived from the thermodynamic fluctuation theory. One important advantage of our derivation is that more correlation information has been taken into account through the inhomogeneous density functions, so that it can be employed to describe the elastic properties of confined fluids.

Based on the MFMT and WDA for hard sphere repulsion and long-ranged attraction, respectively, we have constructed the free energy functional for the confined LJ fluid in the slit pore. In the framework of classic DFT, we have calculated the density profile of confined argon under different conditions.

Further, by calculating the modulus of the confined argon, we have investigated the effect of vapor pressure, temperature, and pore width on its bulk modulus. Our results suggest that the occurrence of the capillary condensation in the pore plays an important role in determining the modulus of the confined fluid. On one hand, the local elastic modulus shows inhomogeneous profile, which arises from the inhomogeneity of the particle density. One the other hand, the changes in intensive and extensive qualities of state may exert different influences on the modulus of the confined fluid. When the pore is full of condensed liquid phase, the bulk modulus shows respectively logarithmic and linear dependence on the vapor pressure and temperature, while it can exhibit oscillation as the pore width is changed. In addition, our further investigation on the solvation pressure dependence of the modulus suggests that the Tait–Murnaghan equation for bulk phase is still valid for the confined fluids.

In summary, the present work provides an efficient and unique strategy to investigate the elastic properties of the confined fluids. Based on its validity that has been shown in this work, it is expected that it can be further applied to explore the rich information about the mechanical behavior in nanoscale materials.

References

[1] Huber P 2015 *J. Phys.: Condens. Matter* **27** 103102
[2] Bhatia S K, Bonilla M R and Nicholson D 2011 *Phys. Chem. Chem. Phys.* **13** 15350
[3] Sawa S and Dasgupta C 2016 *J. Chem. Phys.* **145** 054707
[4] Yu Y X, Gao G H and Wang X L 2006 *J. Phys. Chem. B* **110** 14418
[5] Li Y F, Yu Y X, Zheng Y X and Li J D 2010 *Fluid Phase Equilb.* **292** 110
[6] Yu Y X, Li Y F and Zheng Y X 2010 *Chin. Phys. Lett.* **27** 037101
[7] Peng B and Yu Y X 2009 *J. Chem. Phys.* **131** 134703
[8] Long Y, Palmer J C, Coasne B, Śliwinska-Bartkowiak M and Gubbins K E 2011 *Phys. Chem. Chem. Phys.* **13** 17163
[9] Long Y, Palmer J C, Coasne B, Śliwinska-Bartkowiak M, Jackson G, Müller E A and Gubbins K E 2013 *J. Chem. Phys.* **139** 144701
[10] Srivastava D, Santiso E E and Gubbins K E 2017 *Langmuir* **33** 11231
[11] Rickman J M 2012 *Phys. Rev. E* **86** 062501
[12] Gor G Y, Huber P and Bernstein N 2017 *Appl. Phys. Rev.* **4** 011303
[13] Hoang H and Galliero G 2012 *Phys. Rev. E* **86** 021202
[14] Hoang H and Galliero G 2012 *J. Chem. Phys.* **136** 124902
[15] Mittal J, Truskett T M, Errington J R and Hummer G 2008 *Phys. Rev. Lett.* **100** 145901
[16] Nygård K 2017 *Phys. Chem. Chem. Phys.* **19** 23632
[17] Frank M, Drikakis D and Asproulis N 2015 *Microfluid Nanofluid* **19** 1011
[18] Liu L K, Su D, Tang Y J and Fang G Y 2016 *Renewable and Sustainable Energy Rev.* **62** 305
[19] Page J H, Liu J, Abeles B, Herbolzheimer E, Deckman H W and Weitz D A 1995 *Phys. Rev. E* **52** 2763
[20] Schappert K and Pelster R 2008 *Phys. Rev. B* **78** 174108
[21] Schappert K and Pelster R 2011 *Phys. Rev. B* **83** 184110
[22] Schappert K and Pelster R 2013 *J. Phys.: Condens. Matter* **25** 415302
[23] Schappert K and Pelster R 2013 *Phys. Rev. B* **88** 245443
[24] Schappert K, Naydenov V and Pelster R 2016 *J. Phys. Chem. C* **120** 25990
[25] Schappert K, Gemmel L, Meisberger D and Pelster R 2015 *Europhys. Lett.* **111** 56003
[26] Gor G Y, Siderius D W, Rasmussen C J, Krekelberg W P, Shen V K and Bernstein N 2015 *J. Chem. Phys.* **143** 194506
[27] Gor G Y, Siderius D W, Shen V K and Bernstein N 2016 *J. Chem. Phys.* **145** 164505
[28] Dobrzanski C D, Maximov M A and Gor G Y 2018 *J. Chem. Phys.* **148** 054503
[29] Schofield P 1966 *Proc. Phys. Soc.* **88** 149
[30] Fisher I Z 1964 *Statistical Theory of Liquids* (Chicago: The University of Chicago Press)
[31] Evans R 1979 *Adv. Phys.* **28** 143
[32] Hansen J P and McDonald I R 2006 *Theory of Simple Liquids* (London: Academic Press)
[33] Yu Y X and Wu J Z 2002 *J. Chem. Phys.* **117** 10156
[34] Yu Y X 2009 *J. Chem. Phys.* **131** 024704
[35] Liu Y, Liu H L, Hu Y and Jiang J W 2009 *J. Phys. Chem. B* **113** 12326
[36] Landau L D and Lifshitz E M 1986 *Theory of Elasticity* (Oxford: Pergamon Press)
[37] Irving J H and Kirkwood J G 1950 *J. Chem. Phys.* **18** 817
[38] Barker J A and Henderson D 1967 *J. Chem. Phys.* **47** 4714
[39] CottermanR L, Schwarz B L and Prausnitz J M 1986 *AIChE J.* **32** 1787
[40] Kolafa J and Nezbeda I 1994 *Fluid Phase Equilb.* **100** 1
[41] Heyes D M and Aston P J 1994 *J. Chem. Phys.* **100** 2149
[42] Zwanzig R and Mountain R D 1965 *J. Chem. Phys.* **43** 4464
[43] Steele W A 1973 *Surf. Sci.* **36** 317
[44] Snook I K and van Megen W 1980 *J. Chem. Phys.* **72** 2907
[45] Lakes R and Wojciechowski K W 2008 *Phys. Stat. Sol.* **245** 545
[46] Vakarin E V, Duda Y and Badiali J P 2006 *J. Chem. Phys.* **124** 144515
[47] Murnaghan F D 1944 *Proc. Natl. Acad. Sci. USA* **30** 244
[48] Gor G Y and Neimark A V 2010 *Langmuir* **26** 13021
[49] Gor G Y and Neimark A V 2011 *Langmuir* **27** 6926